Available online at www.sciencedirect.com
ScienceDirect
Journal of Power Sources 179 (2008) 42–49
JOURNAL OF POWER SOURCES
www.elsevier.com/locate/jpowsour

Effect of the catalyst composition in the $Pt_x(Ru–Ir)_{1-x}$/C system on the electro-oxidation of methanol in acid media

K.I.B. Eguiluz, G.R. Salazar-Banda, D. Miwa, S.A.S. Machado, L.A. Avaca *

Instituto de Química de São Carlos, Universidade de São Paulo, C.P. 780, 13560-970 São Carlos, SP, Brazil

Received 23 October 2007; received in revised form 18 December 2007; accepted 19 December 2007
Available online 27 December 2007

Abstract

The effect of variations in the composition for ternary catalysts of the type $Pt_x(Ru–Ir)_{1-x}$/C on the methanol oxidation reaction in acid media for x values of 0.25, 0.50 and 0.75 is reported. The catalysts were prepared by the sol–gel method and characterized by X-ray diffraction (XRD), transmission electron microscopy (TEM), atomic absorption spectroscopy (AAS) and energy dispersive X-ray (EDX) analyses. The nanometric character (2.8–3.2 nm) of the sol–gel deposits was demonstrated by XRD and TEM while EDX and AAS analyses showed that the metallic ratio in the compounds was very near to the expected one. Cyclic voltammograms for methanol oxidation revealed that the reaction onset occur at less positive potentials in all the ternary catalysts tested here when compared to a $Pt_{0.75}$–$Ru_{0.25}$/C (E-Tek) commercial composite. Steady-state polarization experiments (Tafel plots) showed that the $Pt_{0.25}(Ru–Ir)_{0.75}$/C catalyst is the more active one for methanol oxidation as revealed by the shift of the reaction onset towards lower potentials. In addition, constant potential electrolyses suggest that the addition of Ru and Ir to Pt decreases the poisoning effect of the strongly adsorbed species generated during methanol oxidation. Consequently, the $Pt_{0.25}(Ru–Ir)_{0.75}$/C composite catalyst is a very promising one for practical applications.
© 2007 Elsevier B.V. All rights reserved.

Keywords: Methanol oxidation; Direct methanol fuel cells; Electrocatalysis; Sol–gel

1. Introduction

The need for more efficient energy conversion systems is a strong reality for two important reasons, namely, the future shortage of fossil fuel sources as well as the urgency in reducing the contamination levels produced by the use of those fuels in urban centers. In this sense, fuel cells are very promising energy sources due to the high efficiency of the electrochemical combustion in comparison with the chemical combustion thus minimizing the formation of by-products that pollute our planet. Among the different systems under investigation, the use of methanol as the fuel has been the subject of numerous studies since considerable advances have been achieved using that material [1–9].

Although the use of methanol as a fuel is attractive in terms of its theoretical energy density (6.09 kWh kg^{-1}) and theoretical efficiency (96.7%), high overpotentials at both the anode and the cathode reduce the cell potential to 0.51 V and the overall efficiency to ∼41%. Moreover, the formation of CO poisons the Pt-based anode and further reduces the overall efficiency to ∼27%, thereby making CO poisoning one of the major limitations for the technological development of direct methanol fuel cells (DMFCs) [10].

Among the precious metals, Pt shows the highest activity for the electro-oxidation of methanol but the performance of pure Pt electrodes is not very satisfactory due to the formation of strongly adsorbed intermediates. Efforts to reduce the amount of adsorbed CO are centered on the use of co-catalysts and, to date, the addition of ruthenium into the platinum catalyst has yielded the best reported results [11–13]. When binary catalysts are used in DMFCs, the beneficial effect of the second metal M in Pt–M is attributed to a bi-functional mechanism originally proposed by Watanabe and Motoo [2]. There, Pt sites serve to adsorb and dehydrogenate the methanol molecules while M provides nucleation sites for OH_{ads} formation, but the Pt sites become blocked by adsorbed CO making the overall reaction fairly slow. Then, the reaction between $CO_{ads(Pt)}$ and $OH_{ads(M)}$ accelerates again

* Corresponding author. Tel.: +55 16 3373 9943; fax: +55 16 3374 2565.
E-mail address: avaca@iqsc.usp.br (L.A. Avaca).

0378-7753/$ – see front matter © 2007 Elsevier B.V. All rights reserved.
doi:10.1016/j.jpowsour.2007.12.070

the oxidation of methanol by removing the poisoning carbon monoxide.

The bi-functional mechanism is widely accepted at present [6,8,14–17] but an alternative or complementary explanation is the so-called "ligand effect" [18] where M has an influence in the Pt–CO interaction by affecting the electronic structure of the binding site. The latter mechanism has also been supported by electrochemical experiments [19–21], and it has been suggested that the bi-functional mechanism should be modified to account also for electronic effects [20].

Gurau et al. [22] reported that the Ir–O bond is relatively weak and similar in strength to Pt–O while the Ir–C bond is quite strong and close in strength to Pt–C. These authors studied the methanol oxidation on Pt–Ru–Os–Ir alloys and concluded that the addition of Ir appears to accelerate the activation of the C–H bonds in methanol and this behavior is consistent with the substantial literature on C–H activation by Ir and Rh compounds [23–25]. Liang et al. [26] prepared carbon-supported PtRuIr catalyst using a microwave-irradiated polyol plus an annealing synthesis strategy. The PtRuIr/C catalyst displayed a greatly enhanced activity for CO_{ads} electro-oxidation, even higher than that observed on a PtRu/C commercial catalyst (E-Tek). These authors suggested that the superior performance of the PtRuIr/C catalyst must result from the iridium additives, particularly IrO_2. It was also observed an excellent electrocatalytic activity of the carbon-supported PtRuIr nanocomposite for the hydrogen oxidation reaction in the presence of CO [26].

Sivakumar and Tricoli [27] prepared Pt–Ru–Ir nanoparticle catalysts on carbon black using a vapor deposition method. The electrocatalytic activity of the particles towards methanol oxidation was investigated by cyclic voltammetry, chronoamperometry and adsorbed CO-stripping voltammetry and was found that these catalysts possess outstanding activity for methanol oxidation when compared to a Pt–Ru catalyst. CO-stripping voltammetry showed that the superior activity comes partly from a larger active surface area and partly from a higher catalyst resistance to CO poisoning due, in turn, to the presence of iridium.

Besides the chemical nature of the components, the preparation method is another essential parameter in the development of catalysts. Catalysts to be used in fuel cells are normally prepared in the form of particles dispersed onto a high surface area carbon. Several methods have been used to anchor the catalyst particles to the substrate, including the chemical reduction of inorganic salts containing the metals of interest with formic acid [28] and the Bönnemann's method [29]. This latter method involves the reduction of an appropriate inorganic metal salt, by an organic reductive medium (alkali hydrotriorganoborates). The Bönnemann's method appears to be very attractive since it allows the production of nanostructured particles having well-controlled sizes, an essential feature in the production of catalysts. However, the method is rather complicated, involving several steps and the use of sophisticated apparatus.

An attractive alternative to produce catalysts with the desired features is the sol–gel method that has been recently reported as an efficient, simple and low cost way to synthesize very active catalysts for the oxidation of methanol [7,9,30,31]. The sol–gel method is very suitable to prepare pure and homogeneous metals and/or metal oxides [7] with high surface area. Moreover, the sol–gel method allows the production of materials with complex compositions in a very simple and straightforward way. Investigations on a variety of binary and tertiary catalysts for methanol oxidation prepared by sol–gel are being carried out in this laboratory.

The aim of this work is to report the effect of composition in the catalyst system $Pt_x(Ru–Ir)_{1-x}/C$ on the methanol electro-oxidation in acid media since its behavior is much superior than other binary and/or tertiary systems under investigation. The experimental techniques used for this purpose were cyclic voltammetry, quasi-steady-state polarization curves (Tafel plots) and controlled potential electrolysis. The developed Pt/C catalysts modified by the incorporation of different quantities of other metals such as Ru and/or Ir using the sol–gel method were initially characterized by X-ray diffraction (XRD), energy dispersive X-ray (EDX) analysis, atomic absorption spectroscopy (AAS), transmission electron microscopy (TEM) and cyclic voltammetry (CV). Additionally, the catalytic performance of the composite electrodes prepared in this work was compared with that obtained for commercially available Pt/C and $Pt_{0.75}–Ru_{0.25}/C$ catalytic powders using the electrochemical experiments and total organic carbon (TOC) analyses.

2. Experimental

The catalysts were prepared by the sol–gel method using a commercial Pt/C (E-Tek Inc., USA) powder containing 10% of platinum as substrate. Ir and Ru and their mixtures were deposited by dissolving the metallic precursors (ruthenium and iridium acetylacetonates) in a solvent containing isopropanol and acetic acid 3:2 (v/v). After that, an appropriate amount of Pt/C was added to the resulting sol and the mixture was homogenized by ultrasonic irradiation (20 kHz) produced by a Heat System Ultrasonic W85 Sonicator by 30 min. The solvent was then slowly evaporated and the resulting powder submitted to a thermal treatment at 400 °C in an inert Ar atmosphere for 60 min. The desired amount of modifiers was calculated in relation to the amount of platinum in the powder. Binary composites having either Ru or Ir deposited onto Pt/C were prepared using a 1:1 atomic ratio. The ternary composites were prepared having a fixed atomic relationship between the metals Ru and Ir (50:50) and varying the atomic relationship between Pt and the mixture of the metals Ru and Ir. Thus, the catalysts prepared in this work were $Pt_{0.50}–Ru_{0.50}/C$, $Pt_{0.50}–Ir_{0.50}/C$, $Pt_{0.25}(Ru–Ir)_{0.75}/C$, $Pt_{0.50}(Ru–Ir)_{0.50}/C$ and $Pt_{0.75}(Ru–Ir)_{0.25}/C$. For comparison, some experiments were also carried out using Pt/C and $Pt_{0.75}–Ru_{0.25}/C$ from E-Tek.

The physical characterization of the catalysts was initially performed by XRD in a universal diffractometer Carl Zeiss-Jena, URD-6, operating with Cu Kα radiation (λ = 0.15406 nm) generated at 50 kV and 100 mA. The scans were carried out at $1^\circ\ min^{-1}$ for 2θ values between 5° and 100°. This was followed by EDX measurements in a LEO Mod. 440 spectrophotometer with a silicon–lithium detector having a Be window and applying 113 eV and by AAS in a Hitachi Z-8100 spectrophotometer.

The XRD patterns were also analyzed by the software Winfit 1.2 [32] to determine the mean size of the catalysts crystallites. In addition, TEM images were taken using a Philips CM200 microscope operating at 200 kV, coupled to a high-resolution energy dispersive X-ray analysis spectrometer: detector EDX Princeton Gamma Tech PGT Prism. The samples for the TEM and high-resolution EDX analyses were prepared by ultrasonically dispersing the catalyst powders in ethanol. A drop of the suspension was applied onto a carbon-coated copper grid and was dried in air. Samples studied by EDX coupled to a MEV apparatus were prepared by fixing a proper amount of the catalysts powders onto an aluminum substrate using a conducting tape and scanning a ~0.5 cm^2 area every time.

The working electrodes were constructed using the thin porous coating (TPC) configuration [33]. A pyrolitic graphite rod ($\phi = 5$ mm) inserted in a Teflon cylinder and leaving a small cavity (≈0.3 mm) at the end was used to support the catalysts. The working electrodes were prepared by mixing the catalyst powders with a dilute suspension (≈2%, w/w) of a Teflon emulsion (Du Pont TM30) and then following the procedures described elsewhere [33]. All electrochemical measurements were carried out using the TPC electrode configuration. A three-electrode two-compartment Pyrex® glass cell was used for the electrochemical measurements. The counter electrode was a 2 cm^2 platinum foil and the reference electrode was a hydrogen electrode in the same solution (HESS) that was connected by a Luggin capillary. All the experiments were carried out at room temperature in a H_2SO_4 (Merck®) 0.5 mol L^{-1} aqueous solutions also containing methanol (J.T. Baker®) 0.5 mol L^{-1}. The solutions were prepared with analytical grade reagents without further purification and water supplied by a Milli-Q system from Millipore Inc. and were N_2-saturated prior to the measurements.

The electrochemical experiments were carried out using an Autolab Model PGSTAT 30 potentiostat/galvanostat coupled to an IBM-PC compatible microcomputer. All cyclic voltammetric curves reported here correspond to the stationary responses obtained for electrodes cycled between 50 and 1100 mV versus HESS. The quasi-steady-state polarization curves were carried out in the potentiostatic mode with all data points obtained after 300 s of polarization at each potential. The products resulting from the electrochemical oxidation of methanol were analyzed by measuring the total organic carbon using a Shimadzu TOC-V_{CPH} Analyzer.

3. Results and discussion

3.1. Characterization of the composites

Fig. 1 shows the XRD patterns of the commercial composite Pt/C from E-Tek and of $Pt_{0.50}$–$Ir_{0.50}$/C, $Pt_{0.50}$–$Ru_{0.50}$/C, $Pt_{0.25}(Ru–Ir)_{0.75}$/C, $Pt_{0.50}(Ru–Ir)_{0.50}$/C and $Pt_{0.75}(Ru–Ir)_{0.25}$/C, prepared here by the sol–gel route. As expected, the presence of polycrystalline Pt (JCPDS # 04-0802) is revealed by the peaks in 2θ values at 39.9°, 46.2°, 67.9° and 81.0°, corresponding to the reflection planes (1 1 1), (2 0 0), (2 2 0) and (3 1 1), respectively.

In the diffractograms of the composites containing Ru and/or Ir no peaks corresponding to the metals Ir and Ru were observed.

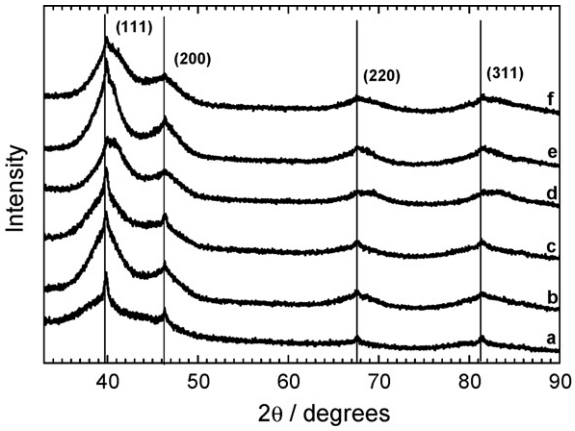

Fig. 1. XRD patterns recorded on catalyst (a) Pt/C from E-Tek, (b) $Pt_{0.50}$–$Ir_{0.50}$/C, (c) $Pt_{0.50}$–$Ru_{0.50}$/C, (d) $Pt_{0.25}(Ru–Ir)_{0.75}$/C, (e) $Pt_{0.50}(Ru–Ir)_{0.50}$/C and (f) $Pt_{0.75}(Ru–Ir)_{0.25}$/C. Vertical lines represent positions of the 2θ values of the peaks of pure Pt.

However, a displacement of the peaks referred to the polycrystalline Pt towards more positive values of 2θ is observed. This can be due to the existence of alloys between the metals Pt, Ru and Ir [27], with a contraction of the crystalline lattice of Pt due to the substitution of some atoms of Pt for the atoms of Ir and/or Ru, that have smaller sizes [34]: ($r_{Ru} = 0.134$ nm) ($r_{Ir} = 0.136$ nm) when compared with Pt ($r_{Pt} = 0.138$ nm) [35].

The XRD patterns (Fig. 1) were also used to estimate the mean crystallite size of the deposited particles on the different materials using the Winfit 1.2 software [32] and the results are presented in Table 1. As previously reported [9,31,36,37], these results show that the sol–gel method is an efficient and very appropriate technique to produce nanometric catalysts with crystallite sizes varying between 2.8 and 3.2 nm.

EDX and AAS analyses were used to determine the composition of the materials prepared by the sol–gel method. Table 1 summarizes the results obtained for the prepared $Pt_{0.50}$–$Ru_{0.50}$/C, $Pt_{0.50}$–$Ir_{0.50}$/C, $Pt_{0.25}(Ru–Ir)_{0.75}$/C, $Pt_{0.50}(Ru–Ir)_{0.50}$/C and $Pt_{0.75}(Ru–Ir)_{0.25}$/C composites. These results show a good agreement between the experimental and the expected theoretical values. Besides high-resolution EDX analysis (Table 1) taken together with the TEM measurements (Fig. 2) and performed in a small area (100 nm^2) have shown that for the $Pt_{0.75}(Ru–Ir)_{0.25}$/C composite, the small and randomly dispersed particles observed (Fig. 2c) are composed by small quantities of Pt (~32%). This deviation from the expected values can be due to the formation of some small Pt agglomerates (~10 nm) also observed in Fig. 2c. This phenomenon was demonstrated by EDX measurements performed only on these agglomerates which are composed preferentially by Pt (~85%). Therefore, the Pt agglomeration could be probably caused by the small quantity of Ru and Ir compounds in the sol–gel solutions. In contrast, the particle segregation observed in the other catalysts should be due to the deposition of Ir and/or Ru compounds on Pt nanoparticles during the sol–gel process thus preventing Pt agglomeration.

Fig. 2 also shows TEM images and their corresponding particle size distribution histograms for the Pt/C (E-Tek),

Table 1
Chemical analysis of the sol–gel prepared catalysts from EDX and AAS measurements, crystallite size calculated from XRD analysis using the Winfit 1.2 program and particle size from TEM

Composite	EDX composition (atomic %)	EDX, high-resolution (atomic %)	AAS composition (atomic %)	Expected composition (atomic %)	Crystallite size (nm)	Particle size (nm), TEM
$Pt_{0.50}$–$Ru_{0.50}$/C	54:46	40:60	53:47	50:50	2.8	2.9 ± 0.814
$Pt_{0.50}$–$Ir_{0.50}$/C	52:48	54:46	51:49	50:50	3.0	3.5 ± 1.130
$Pt_{0.25}(Ru–Ir)_{0.75}$/C	24:40:36	24:44:32	23:39:38	25:37.5:37.5	3.0	2.8 ± 0.772
$Pt_{0.50}(Ru–Ir)_{0.50}$/C	48:27:25	47:28:25	51:26:23	50:25:25	3.2	3.0 ± 0.923
$Pt_{0.75}(Ru–Ir)_{0.25}$/C	72:15:13	32:45:23	73:14:13	75:12.5:12.5	3.2	3.0 ± 0.852

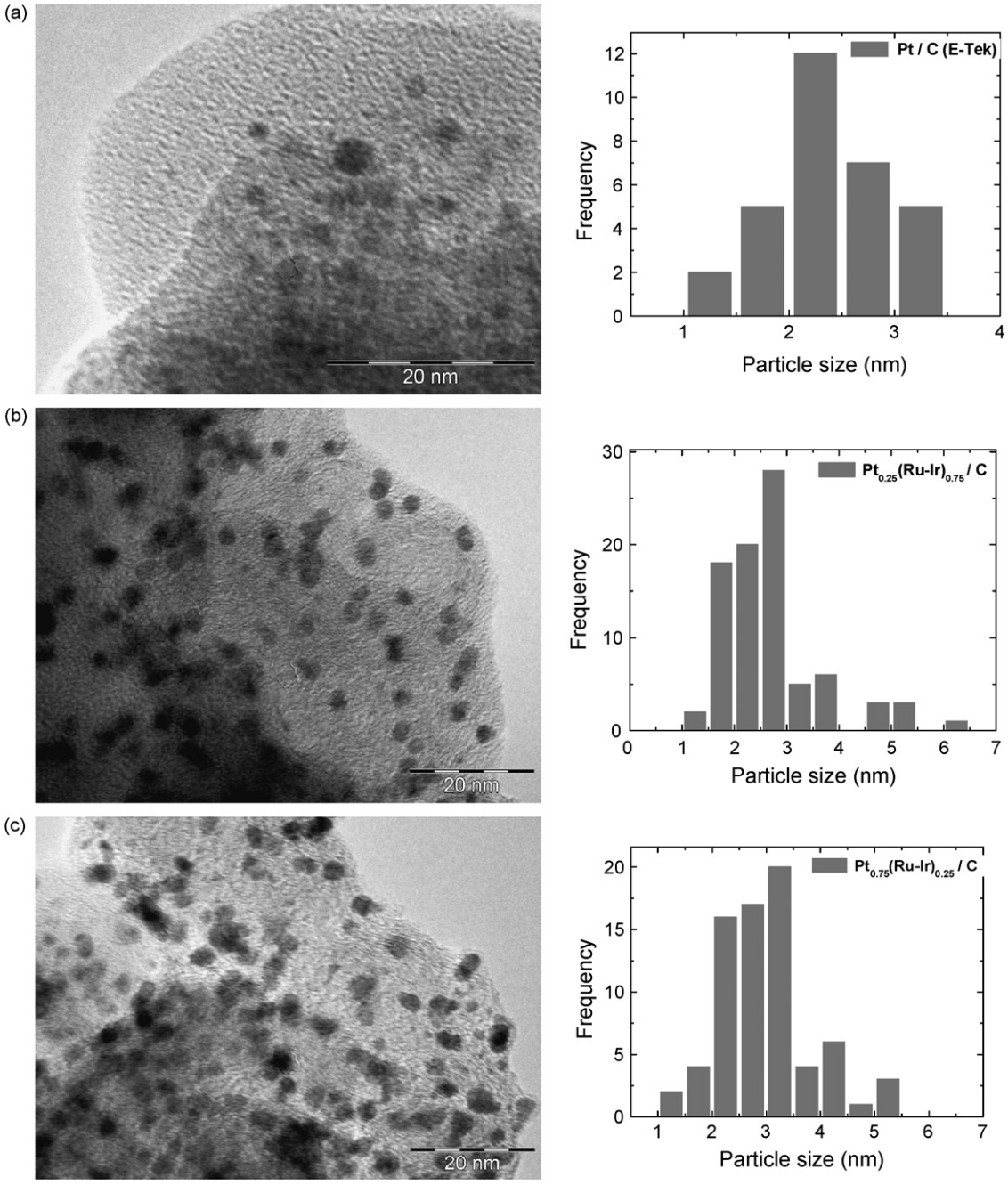

Fig. 2. TEM micrographs and particle size distributions for (a) Pt/C from E-Tek, (b) $Pt_{0.25}(Ru–Ir)_{0.75}$/C and (c) $Pt_{0.75}(Ru–Ir)_{0.25}$/C.

$Pt_{0.25}(Ru–Ir)_{0.75}$/C and $Pt_{0.75}(Ru–Ir)_{0.25}$/C composites. TEM images of the other samples studied here do not show great differences neither in particle size nor in appearance and, therefore, they are not presented. Thus, as it can be seen in that figure, metal nanoparticles are homogeneously dispersed on the surface of the carbon support.

The values of the particle sizes determined from the TEM images and their corresponding standard deviations are also included in Table 1. It is clear from this table that particle sizes observed for the ternary catalyst are small and well-controlled in the range between 2.8 and 3.0 nm. Since the particle sizes of the ternary catalysts are very similar for the different compositions it can be stated that the differences observed for the catalytic activity of these materials (see later) could only be due to their compositions thus revealing a real catalytic effect.

3.2. Electrochemical results

Cyclic voltammograms of electrodes prepared in the thin porous layer configuration and using the different catalysts under investigation were initially recorded at 5 mV s^{-1} in a H_2SO_4 0.5 mol L^{-1} aqueous solution and are presented in Fig. 3. In the absence of methanol, the typical surface processes for polycrystalline Pt such as adsorption/desorption of hydrogen and, to a lower extent, the oxide formation and reduction can be observed in the cyclic voltammogram recorded on the electrode prepared with the Pt/C (E-Tek) composite. The slow scan rate prevented distortions caused by capacitive currents. Thus, using the hydrogen adsorption/desorption charges in the potential range from 0.0 to 300 mV [38], the approximate Pt electroactive surface area was calculated yielding a value of 38.46 cm^2. As the geometric area is 0.19 cm^2, a roughness factor of 196.25 was estimated showing the high active area presented by this electrode, similar to the conditions of an electrode used in a membrane electrode assembly in fuel cells. Meanwhile, the voltammograms corresponding to the $Pt_{0.25}(Ru–Ir)_{0.75}$/C, $Pt_{0.50}(Ru–Ir)_{0.50}$/C and $Pt_{0.75}(Ru–Ir)_{0.25}$/C composites show an inhibition of the hydrogen adsorption/desorption peaks due to the presence of ruthenium [36] and iridium [39] as well as larger currents in the double layer region due to an increase of the capacitive currents and also to Ru and Ir redox processes [39].

It is clear from Fig. 3 that the increase in the currents observed in the double layer region is almost proportional to the increase of the amount of Ru and Ir in the composite. Particularly, the currents are larger on the $Pt_{0.25}(Ru–Ir)_{0.75}$/C composite indicating an area effect for this material. Moreover, it is worth mentioning that no important features could be observed in the CV response of the commercial composite $Pt_{0.75}–Ru_{0.25}$/C (curve not shown), that presents a similar shape to that of the ternary composites shown in Fig. 3 and current values in the same range of those measured for the $Pt_{0.75}(Ru–Ir)_{0.25}$/C (home made) composite.

Methanol oxidation in acid medium on the different electrode materials was initially studied by CV (Fig. 4). The solid curve in Fig. 4 shows that methanol oxidation presents an onset potential of ~335 mV versus HESS on the electrode prepared with the $Pt_{0.25}(Ru–Ir)_{0.75}$/C composite while for the $Pt_{0.50}(Ru–Ir)_{0.50}$/C (dashed line), the $Pt_{0.75}(Ru–Ir)_{0.25}$/C (dotted line) and the $Pt_{0.75}–Ru_{0.25}$/C from E-Tek (dash-dotted line) composites the corresponding potentials are *ca.* 460, 495 and 600 mV versus HESS, respectively (all onset potentials were measured for $j = 10$ A (g Pt)$^{-1}$). It can be also observed that methanol oxidation begins at less positive potentials on the ternary catalysts when compared with the $Pt_{0.75}–Ru_{0.25}$/C (E-Tek) composite, clearly indicating an enhancement of the catalytic activity of the platinum deposit in the presence of both ruthenium and iridium.

Additionally, since the peak current observed for the $Pt_{0.75}–Ru_{0.25}$/C commercial composite (Fig. 4) is somewhat higher than that presented by the $Pt_{0.25}(Ru–Ir)_{0.75}$/C catalyst prepared by the sol–gel method, an area effect cannot be used to explain the superior catalytic activity shown by this sol–gel prepared composite and reflected by the negative shift in the onset potential.

As a result of the different onset potential values for the methanol oxidation reaction (Fig. 4), the pseudo-current density values observed at low potentials on the $Pt_{0.25}(Ru–Ir)_{0.75}$/C

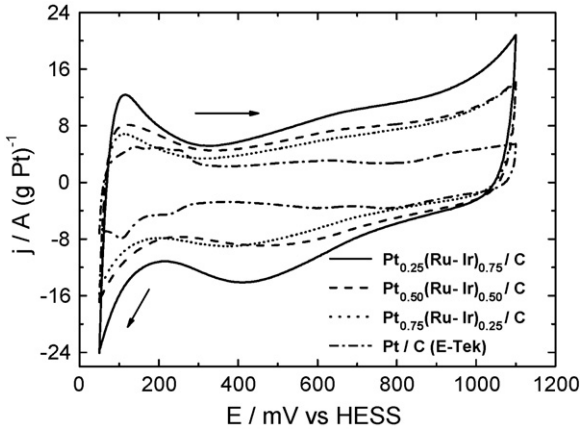

Fig. 3. Steady-state cyclic voltammograms recorded on $Pt_{0.25}(Ru–Ir)_{0.75}$/C (solid line), $Pt_{0.50}(Ru–Ir)_{0.50}$/C (dashed line), $Pt_{0.75}(Ru–Ir)_{0.25}$/C (dotted line) and Pt/C from E-Tek (dash-dotted line), electrodes in 0.5 mol L^{-1} H_2SO_4 aqueous solution ($v = 5$ mV s^{-1}).

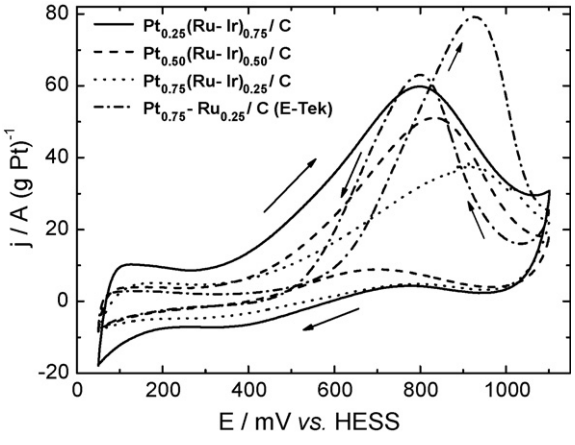

Fig. 4. Cyclic voltammograms (second cycle) for the electrochemical oxidation of methanol 0.5 mol L^{-1} in H_2SO_4 0.5 mol L^{-1} aqueous solution, recorded on $Pt_{0.25}(Ru–Ir)_{0.75}$/C (solid line), $Pt_{0.50}(Ru–Ir)_{0.50}$/C (dashed line), $Pt_{0.75}(Ru–Ir)_{0.25}$/C (dotted line) and $Pt_{0.75}–Ru_{0.25}$/C from E-Tek (dash-dotted line) electrodes ($v = 5$ mV s^{-1}).

composite electrode are higher than those presented by the other catalysts. Therefore, at 500 mV versus HESS, the current density measured for this catalyst is 20 times higher than that observed on the $Pt_{0.75}$–$Ru_{0.25}$/C (E-Tek) composite electrode. In this context, Sivakumar and Tricoli [27] recently reported that the presence of Ir in the catalyst increase the catalytic activity of Pt–Ru–Ir composites towards the methanol oxidation process. These authors observed higher current densities on the catalysts containing Pt–Ru–Ir when compared with a Pt–Ru electrode, particularly for potentials higher than 400 mV versus SHE (standard hydrogen electrode). Likewise, Aramata et al. [40] showed that the species corresponding to suitably oxidized Ir surface states promotes the catalytic activity toward methanol oxidation on Ir electrodes, contributing to the water activation at low potentials (bi-functional mechanism). Furthermore, Gurau et al. [22] concluded that the addition of Ir in Pt–Ru–Os–Ir alloys appears to accelerate the activation of the C–H bonds in methanol, which is consistent with the literature on C–H activation by Ir and Rh compounds [23–25]. Thus, these effects, i.e. a bi-functional mechanism provably presented on Pt–Ir materials added to the activation of the C–H bonds in methanol could explain the results in Fig. 4.

However, due to the different capacitive currents observed for the catalysts by CV (Fig. 4), the use of Tafel plots furnishes a comparison of onset potentials and electrochemical activities in a straightforward manner. Fig. 5 collects the data corresponding to the materials under investigation taken from steady-state polarization curves obtained in the potentiostatic mode after 300 s stabilization at each potential. The onset potentials for methanol oxidation were determined using a fixed pseudo-current density value of $0.2\,A\,(g\,Pt)^{-1}$ and are 230, 276, 282, 405, 417, 484 and 514 mV versus HESS on $Pt_{0.25}(Ru–Ir)_{0.75}$/C, $Pt_{0.50}(Ru–Ir)_{0.50}$/C, $Pt_{0.75}(Ru–Ir)_{0.25}$/C, $Pt_{0.50}$–$Ru_{0.50}$/C, $Pt_{0.50}$–$Ir_{0.50}$/C, $Pt_{0.75}$–$Ru_{0.25}$/C (E-Tek) and Pt/C (E-Tek), respectively. The onset potential values obtained for the ternary catalysts are considerably lower than those reported for the binary ones or even that measured for a commercial Pt–Ru/C catalyst with 40% metal charge [34] in a $HClO_4$ 0.1 mol L^{-1} + CH_3OH 1 mol L^{-1} aqueous solution at 32 °C that yielded ~300 mV versus the reversible hydrogen electrode. These potential values are also lower than the potential reported by Sivakumar and Tricoli [27] on a Pt–Ru–Ir catalyst prepared by the vapor deposition method (i.e. ~380 mV versus SHE).

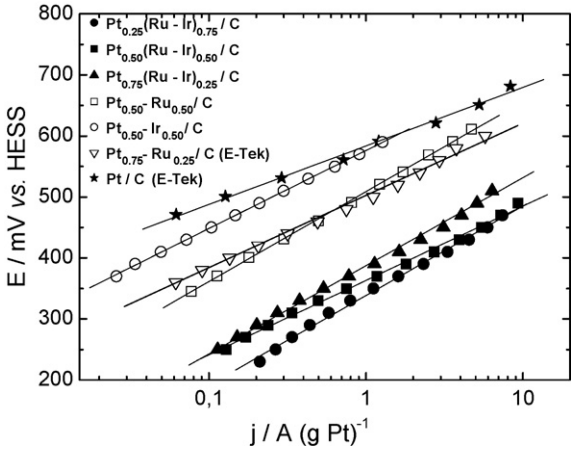

Fig. 5. Tafel plots of the potentiostatic polarization curves performed in quasi-stationary-state for the electrochemical oxidation of methanol 0.5 mol L^{-1} in H_2SO_4 0.5 mol L^{-1} aqueous solution, recorded on the $Pt_{0.25}(Ru–Ir)_{0.75}$/C (●), $Pt_{0.50}(Ru–Ir)_{0.50}$/C (■), $Pt_{0.75}(Ru–Ir)_{0.25}$/C (▲), $Pt_{0.50}$–$Ru_{0.50}$/C (□), $Pt_{0.50}$–$It_{0.50}$/C (◯), $Pt_{0.75}$–$Ru_{0.25}$/C from E-Tek (▽) and Pt/C from E-Tek (⋆) electrodes. All data were obtained from the potentiostatic current decays after 300 s.

The enhancement in the catalytic activity for methanol oxidation presented by the ternary catalysts is clearly observed in Fig. 5. The composite catalyst $Pt_{0.25}(Ru–Ir)_{0.75}$/C shows a shift in the onset potential of about 284 and 187 mV towards less positive potentials when compared with the Pt/C and $Pt_{0.75}$–$Ru_{0.25}$/C commercial composites, respectively. As a consequence, the stationary pseudo-current density determined at a fixed potential of 500 mV is approximately 93 and 13 times higher on $Pt_{0.25}(Ru–Ir)_{0.75}$/C than on the commercial composites, a very important feature for catalysts to be used in practical applications.

Furthermore, it can be observed in Fig. 5 that the sol–gel prepared $Pt_{0.50}$–$Ru_{0.50}$/C composite exhibits a catalytic performance slightly better than that presented by the $Pt_{0.75}$–$Ru_{0.25}$/C from E-Tek, particularly at low potentials (from ~350 to ~450 mV). In view of the fact that the sol–gel method mainly produces ruthenium oxides [9,30], the enhanced catalytic activity observed on the $Pt_{0.50}$–$Ru_{0.50}$/C composite can be probably due to the presence of amorphous ruthenium oxides or hydrous ruthenium oxides which were not detected by the XRD technique. This phenomenon was previously observed on Pt–RuO_2 binary coatings that presented an activity several orders of magnitude larger than the observed on metallic Pt–Ru alloys towards the methanol oxidation reaction [41–43].

On the other hand, the $Pt_{0.50}$–$Ir_{0.50}$/C composite showed a catalytic activity higher than the commercial composite Pt/C proving the synergic effect of the addition of Ir to the Pt, as previously explained in the discussion in Fig. 4. However, its performance is lower than that exhibited by binary catalysts containing Pt and Ru (home prepared and commercial), indicating that the Ru is a better ad-atom for methanol oxidation as recently reported [44].

The Tafel plots shown in Fig. 5 for the methanol oxidation reaction have slopes values between 120 and 140 mV dec^{-1} for all the binary and ternary composites studied. From the kinetic theory of electrode reaction, a Tafel slope of about 118 mV dec^{-1} means that the reaction involving the first electron transfer is the rate-determining step (rds) [45]. Therefore, it can be concluded that the breaking of one of the C–H bonds in the CH_3OH molecule with the first electron transfer is the rate-determining step of methanol electro-oxidation on all catalysts (Eq. (1) in the scheme below) [45]. Meanwhile, the Pt/C (E-Tek) composite presents a Tafel slope of 95 mV dec^{-1} indicating a change in the reaction mechanism for the binary and the ternary catalysts. A Tafel slope of 90 mV dec^{-1} has been already reported on a Pt catalyst and it was suggested that the most likely rds for the methanol oxidation reaction on this material should be the oxidative removal of CO_{ads} by adsorbed intermediates coming from water molecules (Eq. (4)) [46–49]. The overall mechanism

could be represented by

$$Pt\text{–}(CH_3OH)_{ads} \rightarrow Pt\text{–}(CH_3O)_{ads} + H^+ + e^- \quad (1)$$

$$Pt\text{–}(CH_3O)_{ads} \rightarrow Pt\text{–}(CO)_{ads} + 3H^+ + 3e^- \quad (2)$$

$$M + H_2O \rightarrow M\text{–}(OH)_{ads} + H^+ + e^- \quad (3)$$

$$Pt\text{–}(CO)_{ads} + M\text{–}(OH)_{ads} \rightarrow CO_2 + H^+ + e^- \quad (4)$$

where M represents any ad-atom onto the Pt catalyst. Thus, as already demonstrate using spectroscopic techniques [49], the methanol adsorption and dehydrogenation to form CO adsorbed is commonly observed at low potentials for pure Pt. So, the rds for the methanol oxidation on the Pt/C composite is the oxidation of this strongly adsorbed specie (Tafel slope of about 90 mV dec^{-1}). However, the addition of ad-atoms as Ru and/or Ir facilitate the formation of oxygenated species at low potentials (Eq. (3)) [49] and, as a consequence, the oxidation of the CO adsorbed with those species (Eq. (4)) is favored and occurs at lower potentials when compared with pure Pt (bi-functional mechanism) [2]. Consequently, on the binary and ternary catalysts, as the rate of reaction of Eq. (4) is high, the rds of the reaction becomes the methanol adsorption and dehydrogenation represented by Eq. (1) (Tafel slope of about 118 mV dec^{-1}). Note that all the catalysts that contain Pt and Ru and/or Ir in their composition present similar Tafel slopes and so, it is probably that all they work following the bi-functional mechanism but to different extents because of the different onset potentials. These phenomena can be also due to electronic effects on the d-band of the Pt due to the presence of these neighboring ad-atoms [18].

Another important technique for the study of the catalytic activity and surface stability of this kind of electrocatalysts is the use of constant potential electrolysis. The current–time curves presented in Fig. 6 were recorded at a fixed potential of 700 mV versus HESS. As it can be seen in this figure, the slow decrease of the density current observed for the $Pt_{0.25}(Ru–Ir)_{0.75}$ catalyst indicates that this material is poisoning to a lower extend than the others, even for large polarization times (8 h). As a result of that, the stationary pseudo-current density (at 700 mV) at the end of the electrolysis is ∼6 times higher on this catalyst than on $Pt_{0.75}Ru_{0.25}$/C (E-Tek), ∼5 times higher than on $Pt_{0.75}(Ru–Ir)_{0.25}$/C and ∼2 times higher than on $Pt_{0.50}(Ru–Ir)_{0.50}$/C composites. These results suggest that the addition of Ru and Ir to a Pt catalyst decreases the poisoning effect of the strongly adsorbed species generated during methanol oxidation.

Furthermore, during the electrolyses an aliquot of 1 mL was taken from the solution every 2 h for further analysis by TOC. As it can be observed in Fig. 7, after 8 h of electrolysis the composite $Pt_{0.25}(Ru–Ir)_{0.75}$/C presents a drop in the TOC value of 26% which is greater than those for the other composite electrodes (i.e. 18% for the second catalyst in performance, $Pt_{0.50}(Ru–Ir)_{0.50}$). These results could be due to a higher rate in the oxidation of methanol and of the reaction intermediaries occurring on that catalyst thus producing more gaseous CO_2. It is worth noticing that the lowest diminution of the TOC (∼10%) was observed for the $Pt_{0.75}$–$Ru_{0.25}$/C (E-Tek) composite showing that all ternary catalyst prepared in this work present a higher yield for the production of CO_2 than the commercial catalyst. Consequently, they have a better catalytic performance as already observed on the other electrochemical experiments (Figs. 4–6).

It is important to observe that the $Pt_{0.25}(Ru–Ir)_{0.75}$/C catalyst showed the best catalytic performance in the cyclic voltammograms, the Tafel plots and the current–time experiments as well as the highest diminution of TOC (Figs. 4–7). This enhanced catalytic activity could be explained considering that the Ir produces both an acceleration on the activation of the C–H bonds in methanol [22] and a water activation a low potentials (oxides formation) [40]. These effects will be added to the bi-functional mechanism and/or electronic synergic effects presented by the Pt–Ru catalysts. Consequently, this material is a very promising one to be used as catalyst in direct alcohol fuel cell anodes.

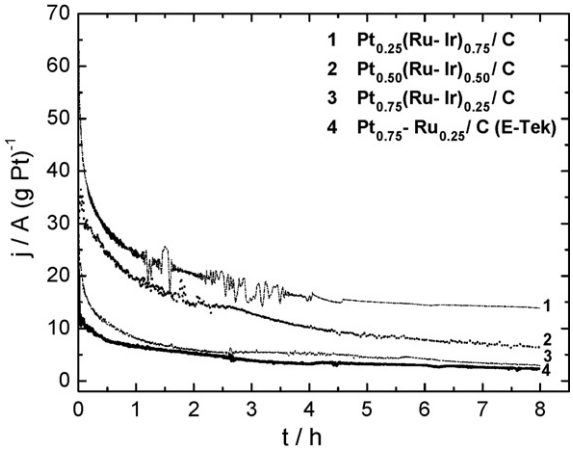

Fig. 6. Current density–time dependence measured at 700 mV vs. HESS fixed potential during 8 h at rotation of 1000 rpm, for the electrochemical oxidation of methanol 0.5 mol L^{-1} in H_2SO_4 0.5 mol L^{-1} aqueous solution, recorded on the $Pt_{0.25}(Ru–Ir)_{0.75}$/C (solid line), $Pt_{0.50}(Ru–Ir)_{0.50}$/C (dashed line), $Pt_{0.75}(Ru–Ir)_{0.25}$/C (dotted line) and $Pt_{0.75}$–$Ru_{0.25}$/C from E-Tek (dash-dotted line) electrodes.

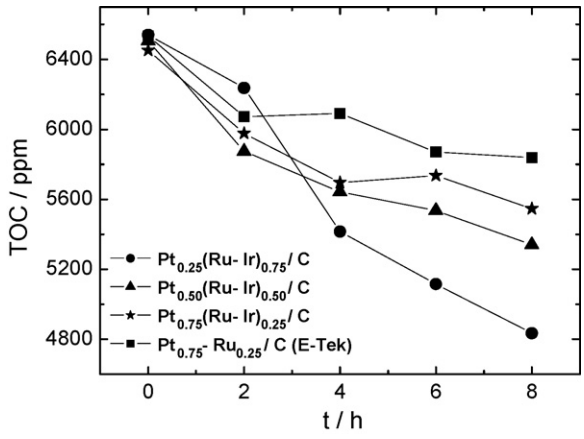

Fig. 7. TOC variation during the electrolyses of Fig. 6 for the catalysts: $Pt_{0.25}(Ru–Ir)_{0.75}$/C (●), $Pt_{0.50}(Ru–Ir)_{0.50}$/C (▲), $Pt_{0.75}(Ru–Ir)_{0.25}$/C (⋆) and $Pt_{0.75}$–$Ru_{0.25}$/C from E-Tek (■).

4. Conclusions

The physical characterization carried out on the $Pt_x(Ru–Ir)_{1-x}$/C ternary catalysts prepared by the sol–gel method showed that this method is a simple and efficient way to produce nanometric deposits with similar particles sizes (between 2.8 and 3.0 nm), homogeneously dispersed on the surface of the carbon supports and with the desired composition.

Cyclic voltammetry and steady-state polarization curves have shown that the composite $Pt_{0.25}(Ru–Ir)_{0.75}$/C has the higher catalytic activity towards methanol oxidation in acid media in comparison to all the other materials studied here. As a consequence, the stationary pseudo-current density measured at a fixed potential of 500 mV is approximately 93 and 13 times higher on that catalyst than on the Pt/C and $Pt_{0.75}$–$Ru_{0.25}$/C commercial composites, respectively. Furthermore, constant potential electrolyses experiments indicate that the $Pt_{0.25}(Ru–Ir)_{0.75}$ catalyst is poisoning to a lower extend than the other catalysts studied, even for long polarization times (8 h). These results suggest that the addition of Ru and Ir to a Pt catalyst decreases the poisoning effect of the strongly adsorbed species generated during methanol oxidation.

Furthermore, the increase in the load of Ru and Ir apparently improves the catalytic performance of those composites. This synergic behavior could be presumably due to the activation of the C–H bonds in methanol and/or the contribution to the water activation at low potentials displayed by Ir compounds plus the bi-functional mechanism and/or electronic effects acting in Pt–Ru catalysts. Consequently, ternary catalysts containing large concentrations of ruthenium and iridium are very promising to be used in anodes of direct methanol fuel cells.

Acknowledgements

The authors wish to thank to the National Research Council-CNPq (Proc. 141421/2004-5) and The State of São Paulo Research Foundation-FAPESP (Proc. 06/50692-2) of Brazil, for the scholarships and financial support to this work.

References

[1] M. Watanabe, S. Motoo, J. Electroanal. Chem. 60 (1975) 267–273.
[2] M. Watanabe, S. Motoo, J. Electroanal. Chem. 60 (1975) 275–283.
[3] V.S. Bagotzky, Yu.B. Vassilief, O.A. Khazova, J. Electroanal. Chem. 81 (1977) 229–238.
[4] J.-M. Leger, C. Lamy, Ber. Bunsenges. Phys. Chem. 94 (1990) 1021–1025.
[5] T. Iwasita, F.C. Nart, W. Vielstich, Ber. Bunsenges. Phys. Chem. 94 (1990) 1030–1034.
[6] H.A. Gasteiger, N.M. Markovic, P.N. Ross Jr., J. Phys. Chem. 99 (1995) 16757–16767.
[7] H.B. Suffredini, V. Tricoli, L.A. Avaca, N. Vatistas, Electrochem. Commun. 6 (2004) 1025–1028.
[8] C. Roth, A.J. Papworth, I. Hussain, R.J. Nichols, D.J. Schiffrin, J. Electroanal. Chem. 581 (2005) 79–85.
[9] G.R. Salazar-Banda, H.B. Suffredini, M.L. Calegaro, S.T. Tanimoto, L.A. Avaca, J. Power Sources 162 (2006) 9–20.
[10] S. Gottesfeld, T.A. Zawodzinski, in: R.C. Alkire, H. Gerischer, D.M. Kolb, C.W. Tobias (Eds.), Advances in Electrochemical Science and Engineering, vol. 5, Wiley–VCH, New York, 1997, pp. 195–197.
[11] X. Ren, M.S. Wilson, S.J. Gottesfeld, J. Electrochem. Soc. 143 (1996) L12–L15.
[12] S. Wasmus, W. Vielstich, J. Appl. Electrochem. 23 (1993) 120–124.
[13] P. Sivakumar, V. Tricoli, Electrochim. Acta 51 (2006) 1235–1243.
[14] E. Ticanelli, J.G. Beery, M.T. Paffett, S. Gottesfeld, J. Electroanal. Chem. 258 (1989) 61–77.
[15] H.A. Gasteiger, N.M. Markovic, P.N. Ross Jr., E.J. Cairns, J. Phys. Chem. 98 (1994) 617–625.
[16] H.A. Gasteiger, N.M. Markovic, P.N. Ross Jr., E.J. Cairns, J. Phys. Chem. 97 (1993) 12020–12029.
[17] R. Ianniello, V.M. Schmidt, U. Stimming, J. Stumper, A. Wallau, Electrochim. Acta 39 (1994) 1863–1869.
[18] M.M.P. Janssen, J. Moolhuysen, J. Catal. 46 (1977) 289–296.
[19] A. Wieckowski, J. Electroanal. Chem. 78 (1977) 229–241.
[20] M. Krausa, W. Vielstich, J. Electroanal. Chem. 379 (1994) 307–314.
[21] Y.Y. Tong, H.S. Kim, P.K. Babu, P. Waszczuk, A. Wieckowski, E. Oldfield, J. Am. Chem. Soc. 124 (2002) 468–473.
[22] B.R. Gurau, R. Viswanathan, R.X. Liu, T.J. Lafrenz, K.L. Ley, E.S. Smotkin, E. Reddington, A. Sapienza, B.C. Chan, T.E. Mallouk, S. Sarangapani, J. Phys. Chem. B 102 (1998) 9997–10003.
[23] A.E. Shilov, Activation of Saturated Hydrocarbons by Transition Metal Complexes, D. Reidel Publishing Company, Dordrecht, Boston, 1984, pp. 24–34.
[24] R.M. Chin, L. Dong, S.B. Duckett, M.G. Partridge, W.D. Jones, R.D. Perutz, J. Am. Chem. Soc. 115 (1993) 7685–7695.
[25] A.A. Bengali, B.A. Arndsten, P.M. Burger, R.H. Schultz, B.H. Weiller, K.R. Kyle, C.B. Moore, R.G. Bergman, Pure Appl. Chem. 67 (1995) 281–288.
[26] Y. Liang, H. Zhang, H. Zhong, X. Zhu, Z. Tian, D. Xu, B. Yi, J. Catal. 238 (2006) 468–476.
[27] P. Sivakumar, V. Tricoli, Electrochem. Solid State 9 (2006) A167–A170.
[28] W.H. Lizcano-Valbuena, V.A. Paganin, E.R. Gonzalez, Electrochim. Acta 47 (2002) 3715–3722.
[29] H. Bönnemann, R. Brinkmann, P. Britz, U. Endruschat, R. Mörtel, U.A. Paulus, G.J. Feldmeyer, T.J. Schmidt, H.A. Gasteiger, R.J. Behm, J. New Mater. Electrochem. Syst. 3 (2000) 199–206.
[30] H.B. Suffredini, V. Tricoli, N. Vatistas, L.A. Avaca, J. Power Sources 158 (2006) 124–128.
[31] M.L. Calegaro, H.B. Suffredini, S.A.S. Machado, L.A. Avaca, J. Power Sources 156 (2006) 300–305.
[32] S. Krumm, Comp. Geosci. 25 (1999) 489–499.
[33] A.A. Tanaka, C. Fierro, D. Scherson, E.B. Yeager, J. Phys. Chem. 91 (1987) 3799–3807.
[34] S.Lj. Gojković, T.R. Vidaković, D.R. Durović, Electrochim. Acta 48 (2003) 3607–3614.
[35] A.J. Dean (Ed.), Lange's Handbook of Chemistry, 13th ed., McGraw-Hill, New York, 1985.
[36] G.R. Salazar-Banda, K.I.B. Eguiluz, L.A. Avaca, Electrochem. Commun. 9 (2007) 59–64.
[37] H.B. Suffredini, G.R. Salazar-Banda, L.A. Avaca, J. Power Sources 171 (2007) 355–362.
[38] H.B. Suffredini, G.R. Salazar-Banda, S.T. Tanimoto, M.L. Calegaro, S.A.S. Machado, L.A. Avaca, J. Brazil. Chem. Soc. 17 (2006) 257–264.
[39] F.I. Mattos-Costa, P. de Lima-Neto, S.A.S. Machado, L.A. Avaca, Electrochim. Acta 44 (1998) 1515–1523.
[40] A. Aramata, T. Yamazaki, K. Kunimatsu, M. Enyo, J. Phys. Chem. 91 (1987) 2309–2314.
[41] D.R. Rolison, P.L. Hagans, K.E. Swider, J.W. Long, Langmuir 15 (1999) 774–779.
[42] J.W. Long, R.M. Stroud, K.E. Swider-Lyons, D.R. Rolison, J. Phys. Chem. B 104 (2000) 9772–9776.
[43] W. Dmowski, T. Egami, K.E. Swider-Lyons, C.T. Love, D.R. Rolison, J. Phys. Chem. B 106 (2002) 12677–12683.
[44] D. Geng, G. Lu, J. Phys. Chem. C 111 (2007) 11897–11902.
[45] N.A. Tapan, J. Prakash, Turk. J. Eng. Environ. Sci. 29 (2005) 95–103.
[46] P.A. Christensen, A. Hamnett, G.L. Troughton, J. Electroanal. Chem. 362 (1993) 207–218.
[47] T.J. Schmidt, H.A. Gasteiger, R.J. Behm, Electrochem. Commun. 1 (1999) 1–4.
[48] S.Lj. Gojković, T.R. Vidaković, Electrochim. Acta 47 (2001) 633–642.
[49] T. Iwasita, Electrochim. Acta 47 (2002) 3663–3674.